The Right-to-Left Shunt of Crocodilians Serves Digestion

C. G. Farmer[1,2,*]
T. J. Uriona[1]
D. B. Olsen[2]
M. Steenblik[1]
K. Sanders[3]
[1]Department of Biology, University of Utah, Salt Lake City, Utah 84112; [2]Utah Artificial Heart Institute, 803N 300W, Suite 180, Salt Lake City, Utah 84103; [3]Department of Radiology, Musculoskeletal Division, University of Utah Health Sciences Center, Salt Lake City, Utah 84132

Accepted 7/17/2007; Electronically Published 1/14/2008

ABSTRACT

All amniotes except birds and mammals have the ability to shunt blood past the lungs, but the physiological function of this ability is poorly understood. We studied the role of the shunt in digestion in juvenile American alligators in the following ways. First, we characterized the shunt in fasting and postprandial animals and found that blood was shunted past the lungs during digestion. Second, we disabled the shunt by surgically sealing the left aortic orifice in one group of animals, and we performed a sham surgery in another. We then compared postprandial rates of gastric acid secretion at body temperatures of 19° and 27°C and rates of digestion of bone at 27°C. Twelve hours after eating, maximal rates of gastric acid secretion when measured at 19° and 27°C were significantly less in the disabled group than in sham-operated animals. Twenty-four hours postprandial, a significant decrease was found at 27°C but not at 19°C. For the first half of digestion, dissolution of cortical bone was significantly slower in the disabled animals. These data suggest the right-to-left shunt serves to retain carbon dioxide in the body so that it can be used by the gastrointestinal system. We hypothesize that the foramen of Panizza functions to enrich with oxygen blood that is destined for the gastrointestinal system to power proton pumps and other energy-demanding processes of digestion and that the right-to-left shunt serves to provide carbon dioxide to gastrointestinal organs besides the stomach, such as the pancreas, spleen, upper small intestine, and liver.

* Corresponding author; e-mail: farmer@biology.utah.edu.

Physiological and Biochemical Zoology 81(2):000–000. 2008. 1522-2152/2008/8102-70162$15.00
DOI: 10.1086/524150

Introduction

The specific aim of this study is to test the hypothesis that the right-to-left shunt of blood past the lungs in American alligators serves digestion by enabling high rates of gastric acid secretion and that this process is highly sensitive to temperature. The broad, long-term objective is to contribute to our understanding of the selective factors that have shaped the cardiopulmonary system of amniotes.

A central problem of the study of the circulatory arrangement of amniotes is understanding the factors leading to the fully divided circulatory systems of birds and mammals and understanding the reasons for the incompletely divided systems of all other members of the group (Goodrich 1930; Ewer 1950; Foxon 1950). One advantage of the divided circulatory system is that high systemic blood pressures can be generated without high pulmonary pressures (which can damage the vasculature in the lungs), and high pressures deliver more blood to tissues for a given resistance to flow. Furthermore, the divided system prevents the mixing of oxygen-rich and oxygen-poor blood. Because a primary function of the cardiorespiratory system is to deliver oxygen to tissues and to carry away carbon dioxide and other "waste" products of metabolism to sites where they can be eliminated from the body (e.g., the lungs, gills, skin, kidneys), the completely divided system seems to have many advantages over the undivided system; so why then is complete separation found in only two groups, both of which are endothermic? Animals with an undivided system can reduce blood flow to the lungs, the primary site of gas exchange in amniotes, and divert this blood back into the systemic circulation, the right-to-left shunt. Are there advantages to this pattern of blood flow, and are there trade-offs or constraints in the evolution of these systems?

Many functions for the shunt have been proposed. Shunting may keep CO_2 out of the lungs during diving, facilitating the uptake of oxygen from the lungs and saving the better-oxygenated blood of the left ventricle for the brain and heart (Greenfield and Morrow 1961; Webb 1979; Grigg 1989). The shunt may suppress metabolism and extend dive times (Hicks and Wang 1999); it may serve thermoregulatory needs (Webb 1979); it reduces pulmonary edema (Burggren 1982); it may facilitate digestion (Jones and Shelton 1993); and it has been hypothesized to speed recovery from a metabolic acidosis by sequestering hydrogen ions (H^+) into the stomach and restoring blood bicarbonate stores (Farmer 2000).

Carbon dioxide is the substrate for the formation of acid in the oxyntic glands of the stomach, and an increase in the partial pressure of CO_2 on the basolateral side of these cells can increase the rate of gastric acid secretion (Kidder and Montgomery 1974; Glauser et al. 1995). Work by Kidder and Montgomery (1974)

suggests that CO_2 diffusion to oxyntic cells is the rate-limiting factor in maximal gastric acid secretion. Thus, theoretically, shunting hypercapnic blood to the stomach could increase the maximal rates of gastric acid secretion over what would be possible from glands perfused with arterial blood. Importantly, gastric acid can be secreted when the oxyntic cells are perfused by the O_2-rich, CO_2-poor blood of the left ventricle, as occurs in all birds and mammals, albeit theoretically at a slower maximal rate.

The crocodilian cardiovascular system is highly suitable for studies of the shunt, which can be stopped by sealing the left aortic orifice. The left aorta is a vessel that arises from the right cardiac ventricle (Figs. 1, 2). The left cardiac ventricle gives rise to a large vessel that subdivides to form the right aorta, the common (primary) carotid, and the right subclavian. After leaving the pericardium, the aortas loop over the primary bronchi and then run caudad to unite by a short, wide connection craniad to the stomach in such a way that the right arch seems to continue on as the dorsal aorta while the left arch seems to continue on as the celiac artery. The celiac branches to supply blood to the stomach, spleen, liver, pancreas, and upper small intestine (Reese 1915). The dorsal aorta supplies blood to the mesenteric artery, the lumbar arteries, the urogenital arteries, and the arteries of the pelvis, hind legs, and tail. Thus, the majority of blood vessels of crocodilians originate from the right-dorsal aorta complex, while the left aorta appears to primarily serve the stomach and other organs of digestion. The left and right aortas have another site of communication, an aperture in the interaortic septum just distal to the bicuspid valves, the foramen of Panizza (Fig. 1*A*). The function of this foramen is unknown.

Crocodilians have significant control over the shunt. The semilunar bicuspid valves are leaflets, and when ventricular pressures exceed arterial pressures, the valves open and blood is ejected into the aortas. However, in addition to these passive, pressure-operated valves, the pulmonary artery of crocodilians has an actively controlled cog-teeth valve. Epinephrine opens the valve, and then right ventricular blood is ejected into the pulmonary artery (Franklin and Axelsson 2000). Acetylcholine, gastrin-releasing peptide, sotalol (an antagonist of β-adrenergic receptors), substance P, and histamine cause a portion of the blood in the right ventricle to be ejected into the left aorta, rather than into the pulmonary artery, by either inducing closure of the cog-teeth valve or causing constriction of intrapulmonary vasculature (White 1956; Greenfield and Morrow 1961; White 1969; Grigg and Johansen 1987; Axelsson et al. 1989, 1991; Grigg 1989, 1992; Holmgren et al. 1989; Jones 1996; Hicks 1998; Franklin and Axelsson 2000). Because the blood that crocodilians shunt into the left aorta from the right ventricle has not passed through the lungs, it is rich in H^+ and CO_2 but poor in O_2, compared with blood that has passed through the lungs. Thus, the left aorta appears to serve as a direct and substantial conduit to shunt CO_2- and H^+-rich blood past the lungs and to the stomach, pancreas, liver, spleen, and upper small intestine (Reese 1915; Webb 1979; Grigg 1989; Jones and Shelton 1993; Jones 1996). The evolution of this highly specialized cardiovascular system and the great degree of control that crocodilians have over this shunt suggests that this system is uniquely tailored by natural selection to serve important functions, but these functions remain poorly understood.

Material and Methods

Several groups of animals were used in a series of experiments aiming to test the hypothesis that the right-to-left shunt serves digestion and to gain insight into why the ability to shunt is found in ectothermic but not endothermic amniotes. The first step was to determine whether a right-to-left shunt occurs during the postprandial period, because if the shunt does not occur at this time, then it is impossible for it to serve digestion. Five juvenile American alligators were used in these experiments, referred to as the blood flow study. In this study, a single blood flow probe was placed on the left aorta, because in crocodilians it is possible to recognize a right-to-left shunt by this blood flow trace (Shelton and Jones 1991; Jones and Shelton 1993; Jones 1996; Fig. 2*F*). Once it had been established that a shunt occurs throughout the postprandial period, the shunt was disabled to assess the effects of the shunt on gastric acid secretion and, therefore, on digestion and to examine the importance of temperature in these processes.

To disable the shunt, a suture was placed around the left aortic orifice, afferent to the foramen of Panizza (Fig. 1*B*). Catheters of polyethylene tubing were placed in either the right atrium or the right ventricle, and metal sutures were loosely placed around the right and left aortas so that the vessels could be identified under fluoroscopy. The sham surgery entailed placement of the atrial or ventricular catheters and the marking of the aortas, but the left aortic orifice was not sealed. The effect of this occlusion was studied in two ways: (1) by direct measurement of rates of gastric acid secretion and (2) by radiographically following the digestion of bone.

To study preferred body temperature (T_b), programmable temperature data loggers (iButton Thermochrons, DS2422, Maxim Dallas Semiconductors) were placed by oral route into the stomachs of six juvenile alligators ranging in size from 2.3 to 4.1 kg. The temperature sensors have a range of $-40°$ to $+85°C$ and are accurate to $\pm 0.5°C$. Each logger was 1.4 cm in diameter and 1 cm thick. The animals were provided a thermal gradient ranging from 15° to 40°C. These animals had not undergone surgery. After implantation of the probes, alligators were returned to their cage, which was kept in a greenhouse with an air temperature of approximately 23°C. Experimental housing consisted of two tanks joined together; each tank was 1.2 m × 2.4 m × 0.6 m. Fresh tap water constantly flowed through one tank, with a thermal gradient from the top to bottom of the tank ranging from 15° to 19°C. The second tank was dry, and heat lamps created a thermal gradient ranging from 23° to 45°C. The basking areas were large enough for all of the animals to bask simultaneously. The alligators were housed together and were free to move about these thermal

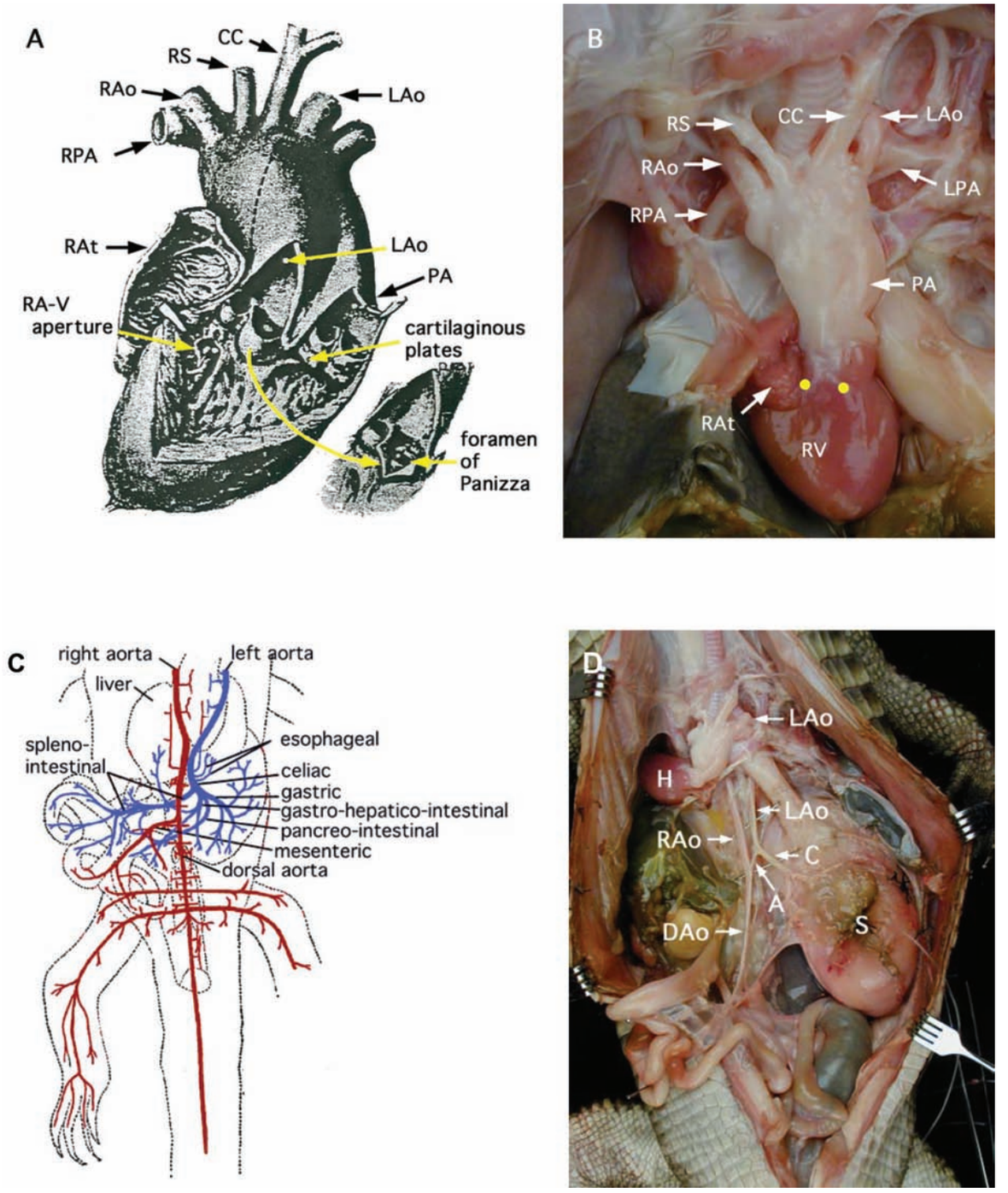

Figure 1. Ventral view of the crocodilian heart, great vessels, and splanchnic circulation. *A*, Schematic of the heart and great vessels (after Greenfield and Morrow 1961). The inset shows an enlargement of a cutaway view of the left aortic orifice. In this illustration, a leaflet of the valve has been split and retracted to reveal the foramen of Panizza. This foramen allows communication between the right and left aortas. *B*, Photograph of a dissection of the heart and great vessels of an American alligator. The yellow dots indicate the approximate location where a suture was placed to occlude the left aorta afferent the foramen. *C*, Schematic of the splanchnic circulation (after Reese 1915). *D*, Photograph of the splanchnic circulation. The left aorta arises from the right cardiac ventricle and can therefore carry O_2-poor, hypercapnic blood, illustrated by blue coloring. The right aorta arises from the left cardiac ventricle and carries O_2-rich but CO_2-poor blood, illustrated by red coloration. The left and right aortas loop over the primary bronchi and then dive dorsad to unite by an anastomosis (*A*) just dorsad to the apex of the cardiac ventricle. Beyond the anastomosis, the vessels align in such a way that the right aorta seems to continue on as the dorsal aorta (*DAo*), while the left arch seems to continue into the celiac artery (*C*). The celiac gives rise to the spleno-intestinal artery, which carries blood to the

gradients. Data collection was postponed for 1 wk after handling. Subsequently core body temperature was recorded every 10 min until the buffer was full, which occurred after 2,048 samples were obtained, 14.2 d after programming. The animals had fasted for 2 wk before being instrumented. Seven days after data collection commenced, the animals were fed ad lib. to satiety on whole mice. At the end of the experimental period, the data loggers were retrieved by gastric lavage. The last 3 d of the fasting period and the first 3 d of the postprandial period were selected for analysis.

Animals

In the blood flow study, American alligators were used that had been hatched in the lab and reared in an animal care facility. In contrast, in the occlusion study and the preferred body temperature study, the animals had been caught from the wild at the Rockefeller Wildlife Refuge by the Louisiana Freshwater Fish and Game Commission. They were transported to Utah. All animals were maintained on a diet of mice in 2.4 × 4.9-m tanks containing areas for swimming and basking. They experienced a natural photocycle. The masses of the animals can be found in Table 1.

Surgery

Before all surgeries, the animals fasted for 1 wk. They were then weighed, anesthetized with isoflurane, intubated, and ventilated (SAR-830, CWE, Ardmore, PA) with air that had passed through a vaporizer (Dräger, Lubeck, Germany). The vaporizer was initially set to 4% isoflurane to induce a surgical plane of anesthesia but was reduced to 0.5% and maintained at this level throughout the majority of the surgery. The site where the incision was to be made was scrubbed with Betadine, and the rest of the animal was covered with a sterile drape. The surgical procedures differed between the studies and thus separate descriptions are given below; however, the recovery procedure was the same. The animals were given 2 mo to recover from the surgery. During recovery, the site of incision was treated with topical antibiotics (Neosporin), kept dry, and covered with clean bandages. The animals were also given antibiotics (Baytril) intramuscularly until the incisions were completely healed. There was no sign of infection in any of the animals. The indwelling vascular catheters were flushed every other day with a sterile saline solution containing heparin (10 IU mL^{-1}).

Blood flow through the left aorta. The left aorta was located as it exits the pericardial sac. Here it was cleared of surrounding connective tissue, and a loose-fitting ultrasonic flow probe (Transonic Systems, Ithaca, NY) was placed around the vessel. The caudal end of the sternum was cut approximately 2.54 cm to access the vessel.

Occlusion of the left aorta. Fourteen American alligators were divided into two groups: five alligators underwent sham surgeries, and nine underwent experimental surgeries. The sham surgery consisted of a midline ventral incision to expose the heart and great vessels. The caudal end of the sternum was cut approximately 2.54 cm to expose the vessels. The left and right aortas were cleared, and a metal suture (B&S 22 surgical steel monofilament, 316L stainless steel, Ethicon) was placed loosely around each vessel as a marker. Polyethylene atrial or ventricular catheters (PE-50 with flared end) were placed and secured with purse-string sutures. The catheters were filled with a mixture of heparin (10 IU mL^{-1}) and saline, tunneled subcutaneously, and exteriorized in a dorsal location. The body wall was closed with absorbable suture (0 Dexon II green braided polyglycolic absorbable; Sherwood Medical, St. Louis, MO). The skin was closed with individually placed silk sutures.

In the experimental group, the right aorta was marked with a metal suture, but the left aorta was occluded at two sites. First, the left aorta was cleared efferent from the point at which the left, right, and pulmonary vessels share common walls and occluded with a suture. Second, the fibrocartilaginous supports of the aortic and pulmonary valves were identified visually. A tapered needle was used to place a second silk suture on the cardiac side of this support such that the left aorta was occluded (Fig. 1*B*). Next, the right atrium or right ventricle was randomly selected for catheterization. The catheters were tunneled subcutaneously and exteriorized in a dorsal location. The body wall was closed with absorbable suture (0 Dexon II). The skin was closed with individually placed silk sutures.

Protocol for the Assessment of the Surgical Technique

To assess the effectiveness of the surgical procedure that sealed the left aortic orifice, a 1–3-mL bolus of radio-opaque material (Omnipaque 300 [iohexol]; Novaplus, Amersham Health) was hand injected through the catheters under fluoroscopy. Then an intracardiac injection of acetylcholine (0.2 mg kg^{-1}) was administered via the same catheters, and the flow patterns were studied.

Protocol for the Measurement of Gastric Acid Secretion

Alligators consumed a meal of chopped steak weighing 5% of their mass and were maintained at T_b of 27°C. Steak was chosen

spleen and part of the small intestine. The celiac then divides to give rise to three arteries: the gastro-hepatico-intestinal, carrying blood to the stomach, liver, and small intestine; the pancreo-intestinal, carrying blood to the pancreas and small intestine; and the gastric, carrying blood to most of the stomach. The rest of the gastrointestinal system is supplied blood by the dorsal aorta, through the mesenteric artery and other branches of the dorsal aorta. *CC* = common carotid, *LPA* = left pulmonary artery, *PA* = pulmonary artery, *LAo* = left aorta, *RAo* = right aorta, *RAt* = right atrium, *RA-V aperture* = right atrial-ventricular aperture, *RPA* = right pulmonary artery, *RS* = right subclavian, *RV* = right ventricle, *H* = heart, *S* = stomach.

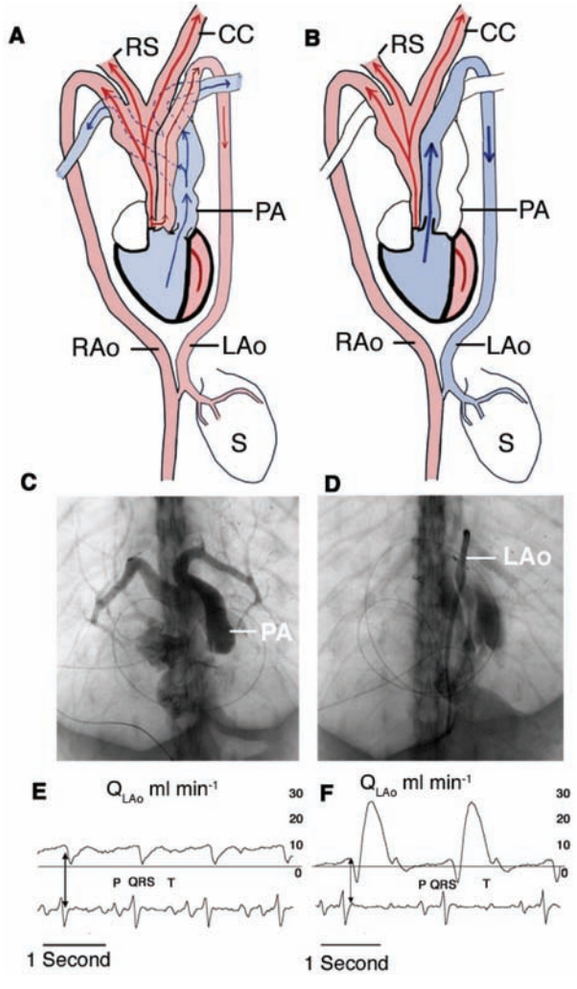

Figure 2. Blood flow through the crocodilian heart without (*A*, *C*, *E*) and with (*B*, *D*, *F*) a shunt. *A*, *B*, Schematic of blood flow. Without a shunt (*A*), the right ventricle (*RV*) ejects O_2-poor, hypercapnic blood (*blue*) into the pulmonary artery (*PA*), while the left ventricle ejects O_2-rich blood (*red*) into the right aorta (*RAo*), which gives rise to many other vessels of the body (e.g., right subclavian [*RS*], common carotid [*CC*]). This oxygenated blood can traverse the foramen of Panizza to flow into the left aorta (*LAo*; Jones and Shelton 1993; Karila et al. 1995; Axelsson and Franklin 1996; Axelsson et al. 1997). With a shunt (*B*), the RV ejects the hypercapnic blood into the LAo, which is continuous with the celiac and gastric arteries. *C*, *D*, Radiographic images of blood flow patterns. Both images show the vessels receiving boli (1–3 mL) of radio-opaque material (Omnipaque 300, iohexol; Novaplus, Amersham Health) that had been infused into the RV. *C*, The RV ejected contrast medium into the PA (no shunt). *D*, Infusion of acetylcholine (0.2 mg kg^{-1} animal weight; Jones and Shelton 1993) into the RV induced a shunt and caused contrast material to be ejected into the LAo. Animals that had the base of the LAo occluded showed no sign of contrast medium in the LAo on infusion of acetylcholine and contrast medium. *E*, *F*, Representative traces from a flow probe (Transonic, Ithaca, NY) that was placed around the LAo (Q_{LAo}) and the electrocardiogram (*bottom trace*). *E*, The flat trace (no shunt) indicates flow from the RAo into the LAo through the foramen of Panizza (Jones and Shelton 1993). *F*, With a shunt, the trace consists of a large pulse indicative of direct ejection from the RV into the LAo. *S* = stomach, Q_{LAo} = blood flow in the left aorta.

instead of mice to avoid hair in the stomach. Although we found that the postprandial preferred body temperature is 30°C, pilot experiments indicated that the alligators would not sit still for an hour at this temperature to have their rates of gastric acid secretion measured. Thus, we chose a cooler temperature to reduce their activity. Twelve and 24 h after the alligators ate, we inserted a solid-state pH electrode (Medtronics) orally into the stomach to measure rates of acid secretion for 1 h by titration with $NaHCO_3$(Fordtran and Walsh 1973). Two weeks later, this same procedure was followed, except the body temperatures of the animals were reduced to 19°C for the 1-h measurement periods. During the measurement periods, the body temperatures were recorded with a thermocouple secured inside the cloaca (26.64°C ± 0.78 mean ± SEM, 18.91°C ± 0.056 mean ± SEM). We computed the mean rate of acid secretion that occurred over the 1-h observation period. We then selected the 10-min interval of this hour that had the highest mean rate to determine maximal rates of acid secretion (Fordtran and Walsh 1973).

Protocol for Assessing Rates of Digestion, Using Digital Radiography

Digital radiographs were used to monitor the effects of occlusion of the left aorta on rates of digestion of bone. The alligators were fed a meal containing a single defleshed, skeletally immature bovine caudal vertebra weighing approximately 0.35% of the body mass of the alligator (Table 1) and a mass of raw hamburger containing 27% fat and weighing 5% of the body mass of the alligator. After feeding, the animals were given 20 min in a water bath (30°C) to ensure that they were well hydrated. The animals were then housed separately at 27°C. The first x-rays taken were on the day of feeding. Subsequent images determined the rate of digestion of the bone on days 3, 6, 9, 13, 15, 17, 19, 21, and 23 following feeding. Twice a week the animals were placed for 20 min into a tank of water held at 30°C so that they could drink.

A Siemens Axiom Aristos digital radiography unit was used with standardized imaging parameters to include a subject-object distance of 104 cm, and exposures using 50 kV and 2 mAs (milliamp seconds). The photoreceiver was kept horizontal (standard extremity radiography configuration) so that the experimental subjects could be placed directly on the surface of the receiver. Animals were allowed to rest in the prone position. Collimation was restricted to the transverse width of the animal and included the inferior (posterior) half of the chest and entire pelvis. An experienced musculoskeletal radiologist was present to assess proper positioning and exposure of each image and to repeat the imaging as necessary. Before the transfer of the digital images to the picture archive and communications system (PACS), animal identification numbers were correlated with time index data applied to the individual images by the radiography unit. Once the images were transferred to the PACS, the individual identifier codes were then manually applied to the images along with digital measurement data. The

Table 1: Mass of the animals and the caudal vertebrae used in the left aorta occlusion study

	Animal Mass (g)	Bovine Caudal Vertebra (g)	Meal Mass × Alligator Mass^{-1}	Days to Complete Digestion
Experimental surgery:				
E1	3,300	11.4	.0035	17
E2	3,300	11.5	.0035	15
E5	2,100	8.4	.0040	23
E6	1,500	5.5	.0037	21
E7	2,300	9.4	.0041	21
E8	2,000	7.0	.0035	21
Mean ± SE	2,417 ± 300	8.87 ± .98	.0037 ± .011	19.6 ± 1.23
Sham surgery:				
C1	2,700	9.7	.0036	13
C2	2,500	9.7	.0039	21
C3	2,000	7.9	.0040	21
C5	1,700	6.2	.0036	17
Mean ± SE	2,225 ± 229	8.38 ± .84	.0038 ± .0001	18.0 ± 1.91

Note. No significant difference was found between the mass of the meals, expressed as a percentage of the body weight of the animal, that were fed to the experimental and sham groups ($P = 0.7$, two-tailed t-test assuming equal variance).

final annotated images were then transformed from digital imaging and communications in medicine format (DICOM) to 24-bit BMP and transferred to an individual storage file from which they were finally burned to compact disc.

Data Analysis

Radiographic data from both studies were analyzed with the same procedure. Measurements of the bone were made using digital calipers at a Phillips Inturis PACS workstation that included a high-resolution 4-megapixel monitor (1,536 × 2,048 pixels) made by NEC. The images were displayed two per screen, with the sagittal plane oriented vertically. The images were then magnified twice and run through an edge-enhancing filter to improve the conspicuity of the bone margins. The lightness/darkness as well as contrast of each image was intermittently adjusted for optimum visualization. Because the ingested caudal vertebrae were not uniform cylinders, varying degrees of obliquity and rotation affected their apparent dimension in the dorsal to ventral projection. Measurements were therefore obtained parallel and perpendicular to the long axis of the bones. The long axis was established by placing one of the two Cobb angle lines along the central long axis. The second line of the Cobb angle tool was then moved until the digital angle measurement read 90°, thus setting a reference perpendicular line to the long axis. As these lines could be moved to any part of the image, accurate parallel measurements could be made by placing subsequent linear measurement tools/calipers on or next to these reference lines. Figure 3 shows how the maximum length, maximum width, and minimum width of the ingested vertebrae were measured in relation to the reference lines. The maximum length was measured from the most protuberant surfaces of the epiphyses parallel to the long axis. Due to morphologic and orientational variances, this maximum length was frequently not superimposed on the central long axis. After fragmentation and separation of the epiphyses, the maximum length was measured in the same manner from the most protuberant visible part of the remaining metaphyseal ends. The maximum width was measured from the outer cortical surfaces of the wider metaphyses along the perpendicular reference line. The minimum width was measured from the outer cortical surfaces of the narrowest part of the diaphyses along the perpendicular reference line. In the initial half of the study, the limiting factor for measurement resolution was the pixel dimension of the monitor, which yielded reproducible measurements of ±0.1 mm. In the latter half of the study, decreased conspicuity of the cortical surface from digestion was a larger factor. As the length of the bone shortened, the position of the minimum width measurement shifted. This had the effect of increasing the minimum width measurement as time proceeded during the latter phase of digestion. If the bone assumed an elliptical shape during digestion, the minimum width measurement was dropped altogether and only maximum width and length data were collected.

To minimize the effect of system performance variation on measurement accuracy, we also obtained a maximum pelvic width measurement to be used as a stable length reference. Since this measurement was taken from between the most protuberant lateral acetabular margins, it is referred to as the transacetabular width (TAW). The TAW line generally fell along the intervertebral space of S1 and S2 (Fig. 3). Small degrees of pelvic obliquity did affect the TAW measurement, and it is not clear whether this may have introduced more or less variability to the measurement accuracy than would have been seen with normal fluctuation in the radiography system itself.

The ingested bone measurement data were then converted to a percentage of the TAW measurement obtained on the same day of imaging. Since each animal is similar in body proportion

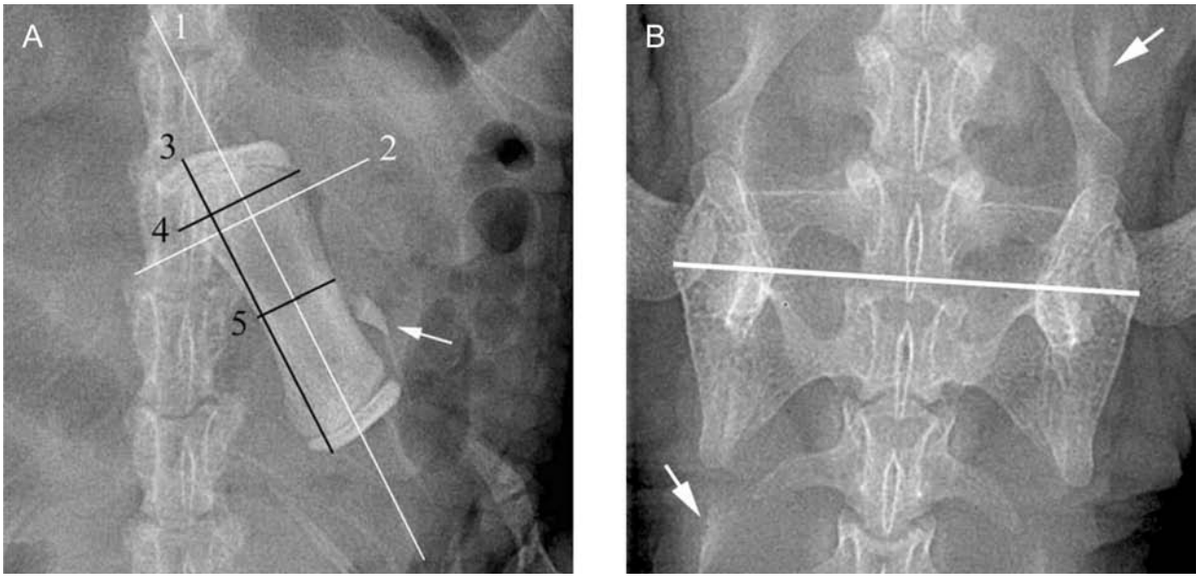

Figure 3. *A*, Radiograph of an ingested vertebra illustrating the measurements taken: *1*, long axis; *2*, perpendicular axis; *3*, maximum length; *4*, maximum width; *5*, minimum width. Note that the maximum length measurement is obtained parallel to but laterally displaced from the long axis reference line in this vertebra with asymmetrical morphology. The arrow indicates an incidentally ingested tooth. *B*, The transacetabular line extends between the most protuberant lateral margins of the acetabula. Note that the line falls over the intervertebral joint of S1 and S2, and the spinous processes of the dorsal-sacral-caudal vertebra are centered on this well-positioned image. Arrows indicate scutes in the lateral row. These scutes may overlie the acetabula and obscure the lateral margins.

despite variation in mass, reporting vertebral measurements as a percentage of TAW had the additional advantage of eliminating scale from the final data pattern.

The distribution of these measurements as percentages of TAW was checked for normality, and a one-tailed Student's *t*-test was used to determine whether the differences seen between the control and experimental groups were significant ($P \leq 0.05$). Once an individual alligator had completed digestion, that animal was no longer included in the analysis.

Results

Preferred Body Temperature

Preferred T_b was significantly greater and less variable after feeding than when fasting; $T_{bfast} = 26.0° \pm 2.02°C$, mean $\pm$ SEM, $N = 6$; $T_{bfed} = 30.10° \pm 0.03°C$ mean $\pm$ SEM, $N = 6$ ($P = 0.0028$, two-tailed *t*-test).

Blood Flow

In all five animals, the right-to-left shunt increased after consumption of a meal. Figure 4 shows representative data collected before and after eating from one animal weighing 2 kg. Each value is the mean rate of shunted blood occurring over a 12-h period.

Gastric Acid Secretion

The peak rates of gastric acid secretion (the maximum mean value occurring during a 10-min interval during a 1-h period of observation) are shown in Figure 5*A*, and mean rates measured over the entire observation periods (1 h each) are shown in Figure 5*B*. ANOVA testing the effects of treatment (occlusion of the left aorta) and temperature on rates of acid secretion at 24 h after eating showed a significant effect of treatment ($F_{1,8} = 18.9$, $P = 0.0024$) and temperature ($F_{1,8} = 9.14$, $P = 0.0165$) as well as a significant interaction between the treatment and temperature ($F_{1,8} = 9.3$, $P = 0.0158$). At 27°C, the control group had significantly greater rates of acid secretion than the experimental group ($\alpha = 0.05$, Bonferroni pairwise comparison of all treatment by temperature effects). No difference between the control ($N = 3$) and experimental ($N = 3$) animals was found at 19°C ($\alpha = 0.05$). There was a significant decrease in rates of acid secretion in the control group at 19°C compared with 27°C and in the experimental group at 19°C compared with 27°C ($\alpha = 0.05$). The sharp decrease in rates of gastric acid secretion at 19°C for the control group suggests this group stopped shunting at the cool temperature.

Left Aorta Occlusion

Assessment of surgical technique. Spot fluoroscopy demonstrated profound bradycardia/transient asystole within 5–20 s of injection of acetycholine, at which time a second contrast bolus was hand-injected. Closure of the pulmonary cog valve and

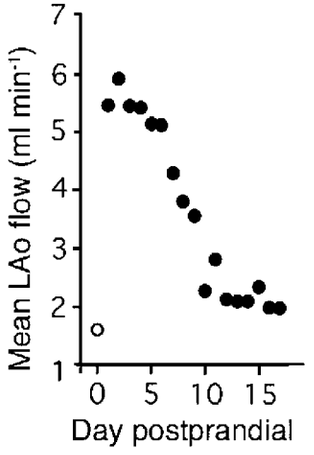

Figure 4. Blood flow through the left aorta (*LAo*) before and after eating, from one alligator that is representative of the five individuals studied. Each symbol is a mean of 12 h of shunted blood flow. *Open circle* = fasting; *filled circles* = postprandial.

pulmonary outflow tract spasm/constriction was observed in all cases. Successful control subjects showed a distinct jet of contrast into the left aorta (shunting; Fig. 2*D*), while successful experimental animals showed pooling of contrast in the right ventricle with intermittent emptying through the pulmonary cog valve and no visualization of the left aorta (left aortic shunt obstructed). Due to the delayed and partial right atrial emptying in subjects with atrial catheters, a greater volume of contrast and more runs were required in those animals with atrial catheters compared to those with ventricular catheters. Atrial runs showed no significant improvement in right ventricular outflow opacification in the supine versus prone position. Right ventricular catheters yielded superior-quality angiograms. Images were captured with a Siemens Axiom Sireskop SD fluoroscope set at 4 frames s^{-1} in angiography (iodine detection) exposure mode. Iohexol doses ranged from a minimum of 5 mL to a maximum of 20 mL. There was no perceivable reaction/irritation to the animal subjects associated with the contrast injections. Experimental animals showing signs of ejection of the radio-opaque material into the left aorta were not included in the study. At the end of the study, the animals were imaged a second time to confirm that the left aorta remained occluded throughout the study.

Out of the nine animals that underwent the experimental surgery, the left aortas of six were successfully occluded, and these animals were used in the study (Table 1). All five of the animals that underwent a sham surgery were initially included in the study. However, toward the end of the study, one of the controls (C-4) bit off and ate the tip of the tail of another alligator during a period in which they were allowed to swim together in the tank of water. Thus, this animal was excluded from the study.

Assessment of rates of digestion. The dissolution and subsequent fragmentation of the ingested vertebrae followed a ste-

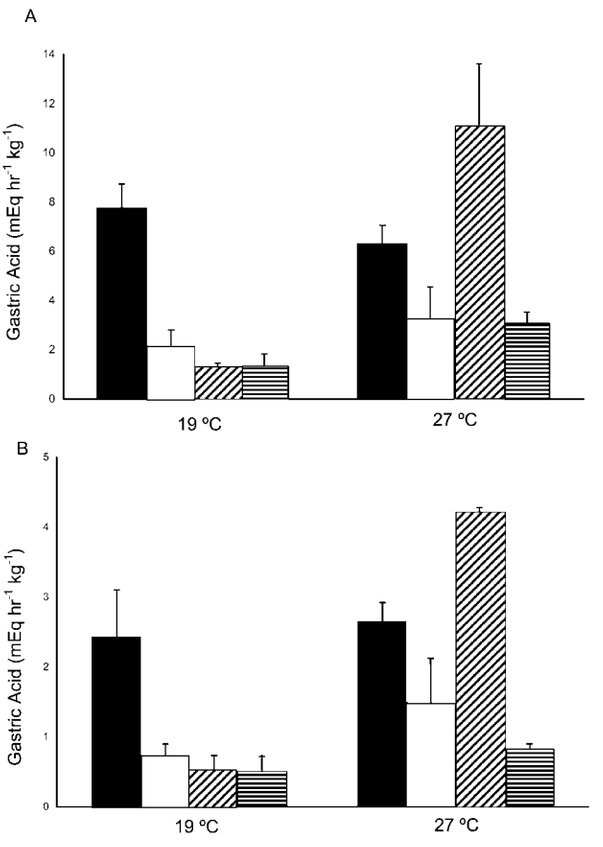

Figure 5. Rates of gastric acid secretion. Measurements were made for 1 h, beginning at 12 (*black bars*) and 24 (*striped bars*) h after the animals consumed a meal of chopped steak. Except during the hour of measurement, the animals were housed at 27°C. The first set of data was collected at 27°C. The animals were given 2 wk rest, and then the experiments were repeated, but during the hour of measurement, body temperature was lowered to 19°C. Body temperature was recorded with a thermocouple secured inside the cloaca (26.64° ± 0.78°C mean ± SE, 18.91° ± 0.056°C mean ± SE). *A*, Means ± SEs of the 10-min periods that gave the largest average rate were included in this analysis. ANOVA testing the effects of treatment (occlusion of the left aorta) and temperature on rates of acid secretion at 24 h after feeding showed a significant effect of treatment ($F_{1,8}$ = 18.9, P = 0.0024) and temperature ($F_{1,8}$ = 9.14, P = 0.0165) as well as a significant interaction between the treatment and temperature ($F_{1,8}$ = 9.3, P = 0.0158). At 27°C, the sham surgery group had significantly greater rates of acid secretion than the occluded group (α = 0.05, Bonferroni pairwise comparison of all treatment-by-temperature effects). After 24 h, no difference between the sham and occluded animals was found at 19°C (α = 0.05). There was a significant decrease in rates of acid secretion in the control group at 19°C compared with rates at 27°C and in the occluded group at 19°C compared with rates at 27°C (α = 0.05). The sharp decrease in rates of gastric acid secretion at 19°C for the shams at 24 h after feeding suggests this group stopped shunting due to the prior exposure to the cool temperature at 12 h postfeeding. *B*, Means ± SEs of the mean rates of acid measured over the entire hour. The solid and striped bars represent measurements made 12 and 24 h after feeding, respectively. Sham surgery group: *black bar* (N = 3), *diagonally striped bar* (N = 3); occluded group: *white bar* (N = 3), *horizontally striped bar* (N = 3).

reotypical sequence (Fig. 6). The first radiographically observable changes included circumferential cortical thinning. As the wider metaphysis anatomically had the thinnest cortex, it was the first point of cortical perforation/fraying. This was closely followed by fraying of the smaller metaphysis. The cartilage-covered epiphyses were least affected in the initial stages of digestion, and maximum length stayed relatively stable for the first half of the digestion sequence, while both maximum and minimum widths decreased at a constant rate. In the last third of the digestion sequence, separation of the epiphyses with fragmentation and continued cortical dissolution resulted in an accelerated decrease in all three dimensions. The shapes of the morphometric curves of this digestion sequence are similar between control and experimental animals as well as between rapid and slow digestors within these cohorts.

No significant differences were seen in the masses of the vertebrae ingested with respect to the alligators' body masses (Table 1). Furthermore, no significant differences in any of the measurements of the vertebrae (maximum width, minimum width, length) were seen on the first or third days after feeding (Fig. 7). Thus, the meals ingested by each group were not significantly different. However, the ways the meals were processed differed between the experimental and control groups. By day 6, a highly significant ($P = 0.002$, one-tailed t-test) difference was found in the maximum width of the vertebrae. Thinning of the bone occurred faster in the control group of animals compared to the experimental (Fig. 7). Significant differences were seen in either the maximum or the minimum measurements from day 6 through day 17 of digestion. However, by day 19, significant differences could no longer be detected (Tables 2, 3, and 4).

The total time required to completely digest the bone was highly variable in each group (Table 1). There was no significant difference between the sham-operated animals and the experimental animals ($P > 0.05$). The experimental animals were slightly larger on average than the controls, and there was a trend for the larger animals to finish digestion more quickly than smaller animals. However, ANCOVA of the mass of the alligator and the time to digest the bone still produced of a P value >0.05.

Discussion

The preponderance of these data indicates that the right-to-left shunt of crocodilians serves digestion. The mechanism remains to be demonstrated, but the shunt probably serves to carry CO_2 to the gastrointestinal tract, where it is then used in the formation of gastric acid. However, all amniotes produce gastric acid, so it is not clear why the shunt is found in ectothermic but not endothermic amniotes. One possibility is that rates of gastric acid secretion are highly dependent on body temperature (T_b), and since ectotherms cannot always maintain preferred T_b, they may need to secrete large amounts of acid while at the appropriate temperature; time is of the essence. In crocodilians, competition for basking sites can be fierce, with larger individuals dominating the sites (Grigg and Seebacher 2000). Basking may also increase small crocodilians' risk of predation, which is extremely high in the first two years of life (Woodward et al. 1987). Thus, it may be especially critical for younger animals to rapidly secrete acid when the opportunity to obtain the requisite T_b arises. In contrast, endothermic lineages can secrete acid independently of environmental temperature fluctuations and basking resources. This hypothesis predicts the following: (1) after feeding, reptiles will bask to increase T_b, (2) rates of gastric acid secretion will be highly sensitive to T_b, and (3) maximal rates of acid secretion will be greater in ectotherms than endotherms when at their respective preferred T_b.

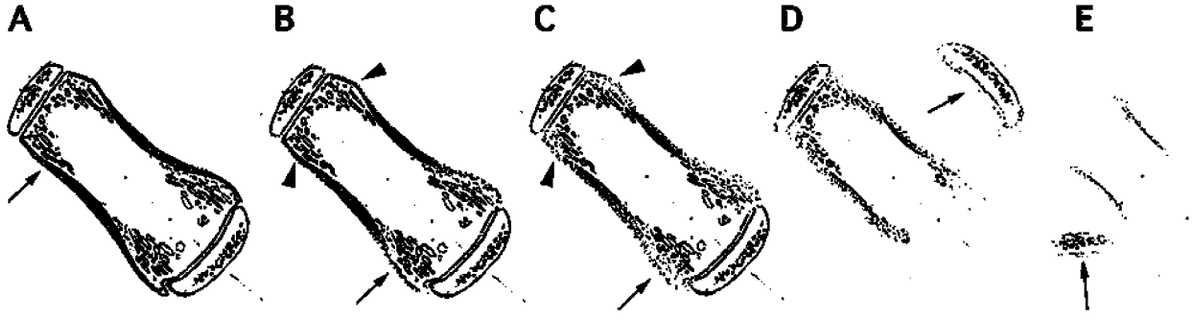

Figure 6. Radiographic appearance of the typical digestion sequence of ingested bovine caudal vertebra. The freshly ingested vertebra displays a distinct and intact cortical surface as indicated by the arrow in *A*. At the end of the first week, cortical erosion is evident along the wider proximal metaphysis (*arrow*) and to a lesser extent in the smaller distal metaphysis (*arrowheads*), as shown in *B*. *C* shows the distinct cortical loss in both metaphyses (proximally, *arrow*, and distally, *arrowheads*), seen at 9–13 d of digestion. At this point, loss of mineralization at the physeal plates is evident and epiphyseal separation is imminent. In *D*, the proximal epiphysis has separated, and there is accelerated erosion of the cortex because the medullary cavity is now exposed to digestive fluids. This radiographic appearance correlates with the rapid increase in digestion rate that marks the slope transition in the last third of the digestion sequence, as depicted by maximum length/width per time graph. *E*, The last visible remnants of the cylindrical vertebral diaphysis and a ghost of the separated distal epiphysis (*arrow*), as seen in the last days of digestion.

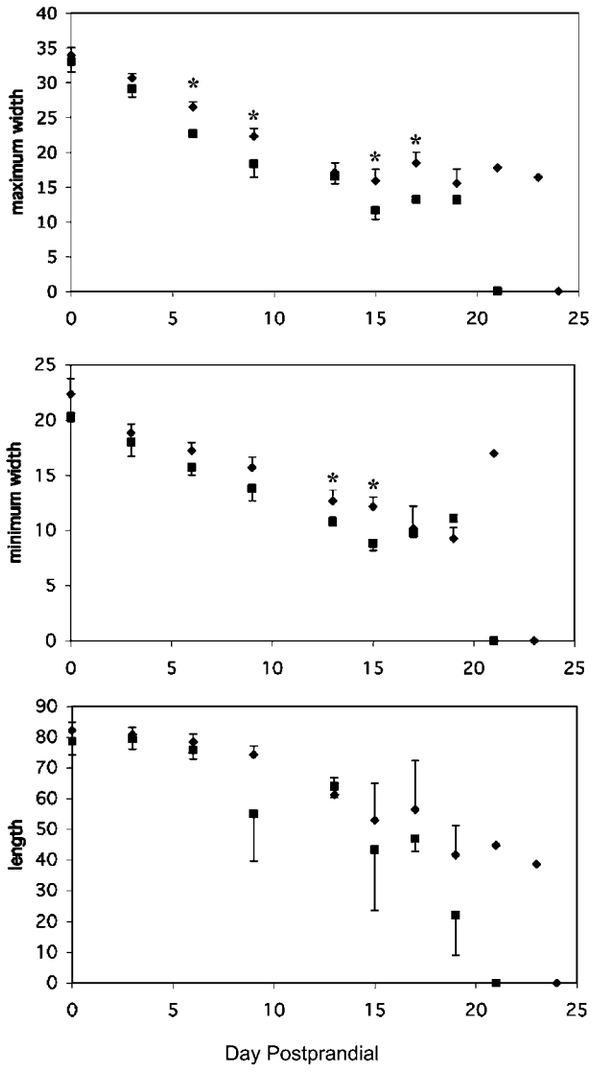

Figure 7. Means ± SEs of the following measurements expressed as a percentage of the transacetabular width: the maximum width of the ingested vertebrae, the minimum width of the ingested vertebrae, and the length of the ingested vertebrae (see Fig. 3). There was no significant difference in these measurements between the control (*squares*) and experimental (*diamonds*) groups when the bones were initially ingested or 3 d after eating. However, by 6 d after feeding, a highly significant difference ($P = 0.0025$, unpaired *t*-test) between the experimental and the control groups was seen in the first part of the bone to show signs of digestion, the thinning of the maximum width of the vertebrae. During this first phase of digestion, the width of the bones thinned at a constant rate. Thus, there was less overall variability in the measurements, and significant differences ($P \leq 0.05$, unpaired *t*-test) between the groups were detected in one or both of the width measurements on days 6, 9, 13, 15, and 17. However, when the epiphases separated, which occurred around day 13, the bones began to fragment, and some of the animals rapidly finished digestion at this point. By day 19, only two animals of the control group retained bone (Tables 1–4), limiting the power of statistical analysis, and on days 21 and 23, no control animals remained, eliminating the ability to statistically analyze the data.

We found that in American alligators, preferred T_b was significantly greater and less variable after feeding than when fasting. Although our results differ from those in prior research, which found no change in preferred body temperature with feeding in a crocodilian (Diefenbach 1975*a*, 1975*b*), in the former study, the animals were handled daily to introduce them to the thermal gradient. If the animals were unaccustomed to this handling, it could have altered their behavior and may explain the discrepancy between the studies. We also found a pronounced decrease in rates of gastric acid secretion with decreasing body temperature. Although we initially attempted to study rates of gastric acid secretion at the postprandial preferred body temperature of 30°C, at this temperature, the animals would not sit still for a 1-h period for observation, and thus we chose to use 27°C. Nevertheless, we measured significantly greater rates of gastric acid secretion at 27°C in both groups of animals. The effect of temperature is more complex than a simple reduction in the turnover rates of enzymes with temperature, because we saw less effect of temperature 12 h into digestion than at 24 h. We suspect the prior cooling at 12 h shut down digestion, and this became apparent in our measurements at 24 h. The exact mechanisms by which this occurs merit further study. Nevertheless, as predicted by the hypothesis, rates of gastric acid secretion are highly sensitive to body temperature. Finally, we found that maximal rates of gastric acid secretion are approximately an order of magnitude greater in our control group of alligators than maximal rates reported for endotherms (postprandial humans with ulcers = 0.9 mEq kg^{-1} h^{-1}; Fordtran and Walsh 1973). Thus, all three predictions of this hypothesis have proven correct.

However, other factors may also be important and may merit investigation. For example, extremely high rates of gastric acid secretion may be especially important for animals that consume large meals. While endotherms tend to eat small but regular meals, many ectotherms consume large meals; for example, American alligators will voluntarily eat meals that weigh 23% of their body mass (Uriona and Farmer 2006). High rates of

Table 2: Mean ± SE of maximum width of the vertebrae as a percentage of transacetabular width in the left aorta occlusion study

Day Postprandial	Experimental		Control	
	Mean ± SE	*N*	Mean ± SE	*N*
0	33.9 ± 1.10	6	33.0 ± 1.47	4
3	30.6 ± .67	6	29.1 ± 1.12	4
6	26.4 ± .80	6	22.7 ± .56	4
9	22.3 ± 1.14	6	18.4 ± 1.95	4
13	17.1 ± 1.37	6	16.6 ± 1.12	3
15	15.9 ± 1.71	5	11.7 ± 1.30	3
17	18.5 ± 1.57	4	13.2 ± .37	2
19	15.6 ± 2.06	4	13.1 ± .65	2
21	17.8 ± .00	1		
23	16.4 ± .00	1		

Table 3: Mean ± SE of minimum width of the vertebrae as a percentage of transacetabular width in the left aorta occlusion study

Day Postprandial	Experimental Mean ± SE	*N*	Control Mean ± SE	*N*
0	22.4 ± 1.39	6	20.4 ± .46	4
3	18.9 ± .78	6	18.0 ± 1.27	4
6	17.2 ± .76	6	15.7 ± .72	4
9	15.7 ± .96	6	13.8 ± 1.10	4
13	12.7 ± 1.03	6	10.8 ± .44	3
15	12.2 ± .90	4	8.8 ± .66	2
17	10.2 ± 2.04	3	9.8 ± .38	2
19	9.3 ± .99	3	11.1 ± 0	1
21	17.0 ± 0	1		

acid secretion may be important for maintaining an acidic gastric environment to prevent putrefaction.

Implications. The role of the shunt in digestion may explain some of the novel and curious features of the crocodilian circulation, including the function of the foramen of Panizza and the allosteric regulation of hemoglobin. Once the acid-producing cells of the stomach have created hydrogen ions, the ions are pumped into the gastric lumen against one of the greatest concentration gradients known to exist in the body of an animal. These pumps require ATP, and thus, the acid-producing cells require oxygen in addition to carbon dioxide. The foramen of Panizza enables boli of O_2-rich blood to flow from the right aorta into the left aorta and thus can enrich left-aortic blood with this much-needed oxygen. Furthermore, unique features of the blood will help unload this O_2 in the gastric circulation. Crocodilian hemoglobin is unusual in decreasing its affinity for O_2 on binding bicarbonate ions (HCO_3^-), rather than on binding molecules of CO_2; chloride ions (Cl^-) competitively bind to the same site (Perutz et al. 1981). Because gastric acid secretion depletes the blood of Cl^- but enriches it with HCO_3^-, this allosteric regulation is suited to unloading O_2 to the acid-secreting glands of the stomach. A digestive function of the shunt also explains the chemical regulation of this blood flow pattern. Many of the neural and endocrine molecules that induce a shunt also promote gastric acid secretion (e.g., acetylcholine, gastrin-releasing peptide, histamine) or have other roles in digestion (e.g., substance P; White 1956, 1969; Greenfield and Morrow 1961; Grigg and Johansen 1987; Axelsson et al. 1989, 1991; Grigg 1989, 1992; Holmgren et al. 1989; Jones 1996; Hicks 1998; Franklin and Axelsson 2000).

Our results have several other implications. First, the right-to-left shunt is probably essential for maximal rates of base production, which are predicted to be equal to the high rates of acid secretion found in our study. The egesta of alligators are not highly acidic (C.G. Farmer, personal observation), and therefore, the large volumes of gastric acid produced must be neutralized in the gastrointestinal system by base. As is the case for gastric acid secretion, maximal rates of base secretion have been shown in studies of mammals to depend on blood-borne CO_2 and cannot occur with the CO_2 available solely from endogenous metabolism of the base-producing cells themselves (Flemstrom and Isenberg 2001; Furukawa et al. 2005). Recall that the left aorta is continuous with the celiac artery, which in turn gives rise to the spleno-intestinal artery (carrying blood to the spleen and part of the small intestine), the gastro-hepatico-intestinal artery (carrying blood to the stomach, liver, and small intestine), and to the pancreo-intestinal artery (carrying blood to the pancreas and small intestine). Thus, maximal rates of base production in the pancreas, liver, and small intestine are probably dependent on the right-to-left shunt.

Furthermore, we hypothesize that this shunt serves to provide carbon to the liver, small intestine, and spleen for the synthesis of glutamine, lipids, uric acid, and hemoglobin. Carboxylation of pyruvate to form oxaloacetate and the subsequent formation of α-ketoglutarate (Delluva and Wilson 1946; Coulson and Hernandez 1983; Stryer 1995) is important to protein metabolism; the α-amino group of many amino acids is transferred to α-ketogluterate to form glutamate. Glutamate can then combine with ammonia to form glutamine. Glutamine plays a key role in integrative metabolism; it is important to acid-base homeostasis and the synthesis of uric acid (Campbell 1991), as a precursor in nucleic acid and nucleotide biosynthesis, in the synthesis of amino sugars, in intraorgan transport (Krebs 1980), and in red blood cell metabolism (Nihara et al. 1998). Coulsen and Hernandez (1983) report that the ability of the liver of lizards to convert CO_2 and pyruvate to glutamine is "without precedence" in that liver glutamine concentrations were increased 30-fold when the animals were given pyruvate. Furthermore, the fixation of CO_2 with pyruvate and the formation of oxaloacetate can be stopped by giving a carbonic anhydrase inhibitor in caimans and lizards (Coulson and Hernandez 1983). Thus, carbonic anhydrase appears to be required for this reaction to occur in vivo. Finally, carbon dioxide is requisite for fatty acid synthesis, a process that begins with the carboxylation of acetyl CoA to form malonyl CoA (Wakil 1989;

Table 4: Mean ± SE of the length of the vertebrae as a percentage of transacetabular width in the left aorta occlusion study

Day Postprandial	Experimental Mean ± SE	*N*	Control Mean ± SE	*N*
0	82.2 ± 2.70	6	78.6 ± 4.49	4
3	80.8 ± 2.38	6	79.5 ± 3.30	4
6	78.45 ± 2.64	6	75.7 ± 2.80	4
9	74.33 ± 2.73	6	55.0 ± 15.41	4
13	61.2 ± 5.54	6	64 ± 3.60	3
15	53.0 ± 12.12	5	43.3 ± 19.57	3
17	56.4 ± 15.83	4	47.0 ± 4.22	2
19	41.6 ± 9.70	4	22.2 ± 13.04	2
21	44.7 ± .0	1		
23	38.6 ± .0	1		

Stryer 1995). This irreversible reaction is the committed step in fatty acid synthesis. In summary, CO_2 is requisite to numerous biochemical processes carried out by the stomach, pancreas, spleen, liver, and small intestine. It is probable that all of these processes are facilitated by blood-borne CO_2. Thus, the hypothesis that the right-to-left shunt of reptiles serves these digestive functions warrants further investigation.

Acknowledgments

We thank J. Hicks and J. Moore for insightful conversations regarding experimental design. We thank F. Adler, M. Butler, D. Feener, and especially I. Terry for advice on the statistical analysis of the data and R. Elsey and staff at the Rockefeller Wildlife Refuge for providing animals. We are grateful to M. Heath and Medtronics for assistance with gastric pH measurements. This work was supported by National Science Foundation grant IBN-0137988 to C.G.F.

Literature Cited

Axelsson M. and C. Franklin. 1996. From anatomy to angioscopy: 163 years of crocodilian cardiovascular research, recent advances and speculations. Comp Biochem Physiol A 118:51–62.

Axelsson M., C. Franklin, R. Fritsche, G.C. Grigg, and S. Nilsson. 1997. The sub-pulmonary conus and the arterial anastomosis as important sites of cardiovascular regulation in the crocodile, *Crocodylus porosus*. J Exp Biol 200:807–814.

Axelsson M., R. Fritsche, S. Holmgren, and D.J. Grove. 1991. Gut blood flow in the estuarine crocodile, *Crocodylus porosus*. Acta Physiol Scand 142:509–516.

Axelsson M., S. Holm, and S. Nilsson. 1989. Flow dynamics of the crocodilian heart. Am J Physiol 256:R875–R879.

Burggren W. 1982. Pulmonary plasma filtration in the turtle: a wet vertebrate lung? Science 215:77–78.

Campbell J.W. 1991. Excretory nitrogen metabolism. Pp. 277–324 in C.L. Prosser, ed. Environmental and Metabolic Animal Physiology. Wiley-Liss, New York.

Coulson R.A. and T. Hernandez. 1983. Alligator metabolism. Comp Biochem Physiol B 74:1–182.

Delluva A.M. and D.W. Wilson. 1946. A study with isotopic carbon of the assimilation of carbon dioxide in the rat. J Biol Chem 166:739–746.

Diefenbach C.O. 1975*a*. Gastric function in *Caiman crocodilus* (Crocodylia: Reptilia). I. Rate of gastric digestion and gastric motility as a function of temperature. Comp Biochem Physiol A 51:259–265.

———. 1975*b*. Gastric function in *Caiman crocodilus* (Crocodylia: Reptilia). II. Effects of temperature on pH and proteolysis. Comp Biochem Physiol A 51:267–274.

Ewer R.F. 1950. Haemodynamic factors in the evolution of the double circulation in the vertebrates. Am Nat 1950:215–220.

Farmer C.G. 2000. Evolution of the vertebrate cardiopulmonary system: new insights. Comp Biochem Physiol B 126(suppl.): 33.

Flemstrom G. and J. Isenberg. 2001. Gastroduodenal mucosal alkaline secretion and mucosal protection. News Physiol Sci 16:23–28.

Fordtran J.S. and J.H. Walsh. 1973. Gastric acid secretion rate and buffer content of the stomach after eating. J Clin Investig 52:645–657.

Foxon G.E.H. 1950. A description of the coronary arteries in dipnoan fishes and some remarks on their importance from the evolutionary standpoint. J Anat 84:121–131.

Franklin C. and M. Axelsson. 2000. An actively controlled heart valve. Nature 406:847–848.

Furukawa O., M. Hirokawa, L. Zhang, T. Takeuchi, L.C. Bi, P.H. Guth, E. Engel, Y. Akiba, and J. Kaunitz. 2005. Mechanism of augmented duodenal HCO_3^- secretion after elevation of luminal CO_2. Am J Physiol 288:G557–G563.

Glauser M., P. Bauerfeind, R. Fraser, and A. Blum. 1995. Regulation of murine acid secretion by CO_2. Pfluegers Arch Eur J Physiol 430:846–851.

Goodrich E.S. 1930. Studies on the Structure and Development of Vertebrates. Macmillan, London.

Greenfield L.J. and A.G. Morrow. 1961. The cardiovascular hemodynamics of Crocodila. J Surg Res 1:97–103.

Grigg G. 1992. Central cardiovascular anatomy and function in Crocodilia. Pp. 339–354 in S.C. Wood, R.E. Weber, A.R. Hargens, and R.W. Millard, eds. Physiological Adaptations in Vertebrates: Respiration, Circulation and Metabolism. Dekker, New York.

Grigg G. and K. Johansen. 1987. Cardiovascular dynamics in *Crododylus porosus* breathing air and during voluntary aerobic dives. J Comp Physiol B 157:381–392.

Grigg G.C. 1989. The heart and flow patterns of cardiac outflow in the crocodilia. Proc Aust Physiol Pharmacol Soc 20:43–57.

Grigg G.C. and F. Seebacher. 2000. Crocodilian thermal relations. Pp. 297–309 in G.C. Grigg, F. Seebacher, and C. Franklin, eds. Crocodilian Biology and Evolution. Surrey Beatty, Chipping Norton, Australia.

Hicks J.W. 1998. Cardiac shunting in reptiles: mechanisms, regulation and physiological function. Pp. 425–483 in C. Gans and A.S. Gaunt, eds. Biology of the Reptilia. Vol. G. Society for the Study of Amphibians and Reptiles, Ithaca, NY.

Hicks J.W. and T. Wang. 1999. Hypoxic hypometabolism in the anesthetized turtle, *Trachemys scripta*. Am J Physiol 277:R18–R23.

Holmgren S., M. Axelsson, J. Jensen, G. Aldman, and K. Sundell. 1989. Bombesin-like immunoreactivity and the effect of bombesin in the gut, circulatory system and lung of the caiman, *Caiman crocodylus crocodylus*, and the crocodile, *Crocodylus porosus*. Exp Biol 48:261–271.

Jones D.R. 1996. The crocodilian central circulation: reptilian or avian? Verh Dtsch Zool Ges 89:209–218.

Jones D.R. and G. Shelton. 1993. The physiology of the alligator

heart: left aortic flow patterns and right-to-left shunts. J Exp Biol 176:247–269.

Karila P., M. Axelsson, C. Franklin, R. Fritsche, I.L. Gibbins, G.C. Grigg, S. Nilsson, and S. Holmgren. 1995. Neuropeptide immunoreactivity and co-existence in cardiovascular nerves and autonomic ganglia of the estuarine crocodile, *Crocodylus porosus*, and cardiovascular effects of neuropeptides. Regul Pept 58:25–39.

Kidder G.W. and C.W. Montgomery. 1974. CO_2 diffusion into frog gastric mucosa as rate-limiting factor in acid secretion. Am J Physiol 227:300–304.

Krebs H. 1980. Special lecture: glutamine metabolism in the animal body. Pp. 319–329 in J. Mora and R. Palacios, eds. Glutamine Metabolism Enzymology and Regulation. Academic Press, New York.

Nihara Y., C.R. Zerez, D.S. Akiyama, and K.R. Tanaka. 1998. Oral L-glutamine therapy for sickle cell anemia. 1. Subjective clinical improvement and favorable change in red cell NAD redox potential. Am J Hematol 58:117–121.

Perutz M.F., C. Bauer, G. Gros, F. Leclercq, C. Vandecasserie, G. Schnek, G. Braunitzer, A.E. Friday, and K.A. Joysey. 1981. Allosteric regulation of crocodilian haemoglobin. Nature 291:682–291.

Reese A.M. 1915. The Alligator and Its Allies. Putnam, New York.

Shelton G. and D.R. Jones. 1991. The physiology of the alligator heart: the cardiac cycle. J Exp Biol 158:539–564.

Stryer L. 1995. Biochemistry. W.H. Freeman, New York.

Uriona T.J. and C.G. Farmer. 2006. Contribution of the diaphragmaticus muscle to vital capacity in post-prandial American alligators (*Alligator mississippiensis*). J Exp Biol 208 3047–3053.

Wakil S.J. 1989. Fatty acid synthase, a proficient multifaunctional enzyme. Biochemistry 28:4523–4530.

Webb G. 1979. Comparative cardiac anatomy of the Reptilia. III. The heart of crocodilians and an hypothesis on the completion of the interventricular septum of crocodilians and birds. J Morphol 161:221–240.

White F.N. 1956. Circulation in the reptilian heart (*Caiman sclerops*). Anat Rec 125:129–134.

———. 1969. Redistribution of cardiac output in the diving alligator. Copeia 1969:567–570.

Woodward A.R., T.C. Hines, L. Abercrombie, and J.D. Nichols. 1987. Survival of young American alligators on a Florida lake. J Wildl Manag 51:931–937.